




# Introduction of the vortex Hermite-Cosh-Gaussian beam and the analysis of its intensity pattern upon propagation

Z. Hricha<sup>1</sup> · M. Yaalou<sup>1</sup> · A. Belafhal<sup>1</sup> 

Received: 2 May 2020 / Accepted: 14 December 2020 / Published online: 22 January 2021  
© The Author(s), under exclusive licence to Springer Science+Business Media, LLC part of Springer Nature 2021

## Abstract

In this paper, a vortex-Hermite-cosh-Gaussian beam (vHChGB) is introduced as a general form of the vortex cosh-Gaussian and vortex Hermite-Gaussian beams. Based on the Huygens-Fresnel diffraction integral, a propagation formula of the vHChGB passing through a paraxial optical system is derived. The evolution of the intensity pattern of the propagated vHChGB as a function of the beam order, decentered parameter ( $b$  parameter) and topological vortex charge is discussed with numerical results. It is shown that the vHChGB shape in the source plane depends crucially on the decentered parameter. In far-field, the multi-lobe profile obtained for small  $b$  evolves into a four-petal-like beam. Whereas the initial four-lobe profile for large  $b$ , morphs into a multi-lobes pattern. The vHChGB shows specific intensity patterns depending on the beam order and the vortex charge. This study may be beneficial for applications involving beam shaping of hollow vortex beam, beam splitting techniques and optical communications.

**Keywords** Hermite-cosh-gaussian beams · Vortex hollow beams · Topological charge · Cosh-gaussian beam · Huygens-fresnel integral transformation

## 1 Introduction

During the last few years, there has been growing interest for the study of dark hollow vortex beams due to their potential applications in various fields, such as optical trapping, optical microscopy, wireless communications and optical micromanipulations (Ito et al. 1996; Kuga et al. 1997; Paterson et al. 2001; Cai et al. 2003; Bishop et al. 2004; Torok and Munro 2004; Cai and Ge 2006; Wang et al. 2012; Rubinsztein-Dunlop, et al. 2017). Several vortex beams which were introduced for the cylindrical symmetry are separable in the polar coordinates, as examples, we cite the well-known Laguerre-Gaussian (Allen et al. 1992; Kennedy et al. 2002; Vallone 2015), Bessel-Gaussian (Arlt and Dholakia 2000;

---

✉ Z. Hricha  
hrichaz@hotmail.com

✉ A. Belafhal  
belafhal@gmail.com

<sup>1</sup> Laboratory LPNAMME, Laser Physics Group, Department of Physics, Faculty of Sciences, Chouaib Doukkali University, P. B 20, 24000 El Jadida, Morocco

McGloin and Dholakia 2005; Kotlyar et al. 2006; Vaity and Rusch 2015), hypergeometric-Gaussian (Kotlyar et al. 2007; Karimi et al. 2007; Skidanov et al. 2013) and flat-topped Gaussian beams (Liu et al. 2015). While, the well-known rectangular laser beams which are separable in the orthogonal direction, such as Hermite sinusoidal-Gaussian (Casperson and Tovar 1998; Tovar and Casperson 1998), four-petal Gaussian (Duan and Lü 2006), Lorentz-Gaussian (Zhou 2010) and Finite Airy beams (Siviloglou et al. 2007; Siviloglou and Christodoulides 2007) are not originally vortex modes but they can be embedded by vortex phase amplitude. The resulting vortex beams can then carry the orbital angular momentum and have specific shape patterns. Some of the beams considered above were generated experimentally by means of laser resonators or diffractive optical elements (Guo et al. 2014; Wang et al. 2019; Kotlyar et al. 2015; Monin and Ustinov 2018; Dai et al. 2010; Zhou and Ru 2013). A kind of hollow vortex-beam, named as hollow vortex-Gaussian beams, has been discovered by Zhou et al. (Zhou et al. 2013, 2018). These beams show a high propagation stability in free space and thus may have potential application in optical micromanipulations. More recently, a vortex cosh-Gaussian beam (vChGB), which is a cosh-Gaussian field embedded with a vortex phase has been proposed to describe a more general type of hollow vortex beams in the rectangular symmetry (Hricha et al. 2020). The proposed model beam has one additional control parameter more than to the simple vortex Gaussian beam. The propagation properties of this beam in free-space and in FrFT system have been investigated in details (Hricha et al. (2020)). In the source plane, the vChGB may resembles to the vortex-Gaussian field for small values of  $b$ , whereas it splits into a four-lobes structure resembling to the four-petal Gaussian beam when  $b$  is large. To extend further our research on rectangular beams carrying vortex phase structure, we propose in this paper a Hermite-cosh-Gaussian beam embedded with a vortex phase, which we will refer to as vortex Hermite-cosh-Gaussian beam (vHChGB). In the source plane, the vHChGB has three key parameters, namely the beam orders ( $p$ ,  $q$ ), the decentered parameter  $b$  and the vortex charge number  $M$ . The high number of the parameter permits to produce a broad variety of beam patterns, and the well-known vortex-Gaussian, vortex Hermite-Gaussian and vortex-cosh-Gaussian beams can be regarded as limiting cases of the vHChGB. The present paper is aimed at investigating the propagation characteristics of the vHChGB passing through a paraxial optical system. The closed-form expression of the propagated vHChGB in a paraxial optical medium is derived based on the Collins formula. The spatial characteristics of the beam are analyzed numerically with illustrated examples. The remainder of the manuscript is organized as follows: in Sect. 2, the vHChGB pattern is illustrated, in the source plane, as a function of the beam parameters. Then in Sect. 3, the propagation formula of the vHChGB through a paraxial ABCD optical system is derived by means of the Huygens-Fresnel diffraction integral. In Sect. 4, the spatial characteristics of the vHChGB in free space are discussed numerically with illustrated examples. The main results are outlined in the conclusion part.

## 2 Characteristics of the vHChGB pattern at the source plane

In the Cartesian coordinates system, the  $z$ -axis is taken to be as the propagation direction. A vHChGB can be for instance generated by using a Hermite-cosine hyperbolic-Gaussian beam (HChGB) (Belafhal and Ibnchaikh 2000; Ibnchaikh et al. 2001; Hricha and Belafhal 2005a, 2005b) in passage through a spiral phase plate (SPP) (Oemrawsingh et al. 2004; Kotlyar et al. 2005). The SPP may modulate the wave-front phase of the field so that the

resulting beam may acquire the orbital angular momentum, which is associated with a vortex charge  $M$  at the beam's center.

The general vHChGB in the source plane  $z=0$  takes the form

$$E_{pq}(x_0, y_0, z=0) = E_p(x_0, z=0) E_q(y_0, z=0) (x_0 + iy_0)^M \quad (1a)$$

where

$$E_j(u, z=0) = H_j\left(\frac{\sqrt{2}u}{\omega_0}\right) \cosh\left(\frac{b}{\omega_0}u\right) \exp\left(-\frac{u^2}{\omega_0^2}\right), \quad (1b)$$

with  $j = p$  or  $q$ , and  $u = x_0$  or  $y_0$ .  $(x_0, y_0)$  being the Cartesian coordinates at the source plane, and  $(p, q)$  are the mode indexes associated with the Hermite polynomials  $H_p(\cdot)$  and  $H_q(\cdot)$  in the  $x$ - and  $y$ -directions, respectively.  $\cosh(\cdot)$  denotes the hyperbolic-cosine function,  $\omega_0$  is the waist size of the Gaussian part,  $b$  is the decentered parameter associated with the cosh part, and the integer parameter  $M$  denotes the topological charge of the spiral phase plate.

From Eq. (1a) one can deduce that the profile of a vHChGB at the source plane is determined by five parameters, i.e.,  $p, q, b, M$  and  $\omega_0$ . By setting particular values of the beam parameters, Eq. (1a) may describe a set of well-known beams, such as the Gaussian beam when  $p = q = M = b = 0$ , hollow vortex-Gaussian beam for  $p = q = b = 0$  (Zhou et al. 2013), vortex-cosh-Gauss beam (vChGB) when  $p = q = 0$  (Hricha et al. 2020), vortex Hermite-Gaussian beam (vHGB) (Kotlyar et al. 2015; Monin and Ustinov 2018) for  $b=0$  and HChG beam for  $M=0$  (Belafhal and Ibnchaikh 2000; Ibnchaikh et al. 2001; Hricha and Belafhal 2005a). With the embedded vortex charge, the vCHGBs can be used as optical traps; they may be able to trap both high- and low-index microparticles as well as to set them into rotation by use of the orbital angular momentum of light.

Equation (1a) can also be rewritten as

$$\begin{aligned} E_{pq}(x_0, y_0, z=0) &= \frac{1}{4} \exp\left(\frac{b^2}{4}\right) H_p\left(\frac{\sqrt{2}x_0}{\omega_0}\right) H_q\left(\frac{\sqrt{2}y_0}{\omega_0}\right) \\ &\times \left\{ \exp\left[-\left(\frac{x_0}{\omega_0} - \frac{b}{2}\right)^2\right] + \exp\left[-\left(\frac{x_0}{\omega_0} + \frac{b}{2}\right)^2\right] \right\} \\ &\times \left\{ \exp\left[-\left(\frac{y_0}{\omega_0} - \frac{b}{2}\right)^2\right] + \exp\left[-\left(\frac{y_0}{\omega_0} + \frac{b}{2}\right)^2\right] \right\} (x_0 + iy_0)^M, \end{aligned} \quad (2)$$

this suggests that the vHChG beam can be obtained by a superposition of four Hermite-decentered Gaussian modes embedded with the same vortex phase.

As a preliminary illustration of vHChG field at the source plane, we depicted in Figs. (1, 2), the intensity distributions of the beam versus the parameters  $(p, q)$ ,  $b$  and  $M$ . For convenience, the waist width is fixed to be  $\omega_0=1$  mm in all calculations.

From the plots of these figures, it is shown that a vHChG field has a multi-petal structure with a dark central region. The shape pattern is mirror symmetric and depends crucially on the value of  $b$  parameter, that is, for small  $b$  ( $b < 1$ ), the beam exhibits  $2(p+q)$  petals (see Fig. 1). The main lobes are located at the vertices of the four-squared beam pattern. While for large  $b$ , the secondary lobes disappear and only the main lobes remain

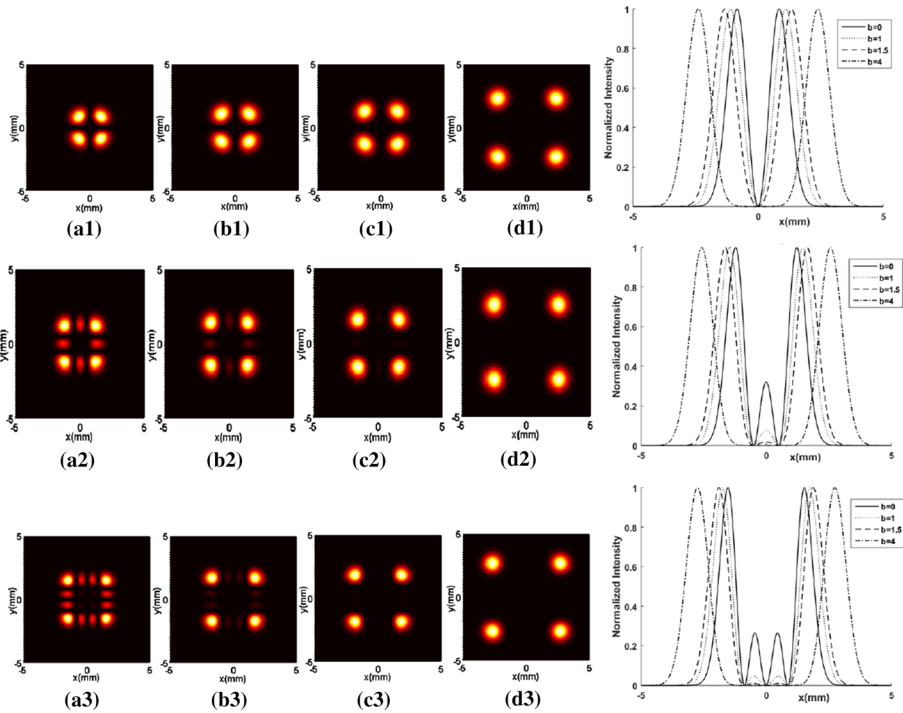


**Fig. 1** The normalized intensity distribution of a vHChG beam at the source plane with  $\omega_0=1$  mm and  $M=1$  for different values of  $(p,q)$  and  $b$ . The top, middle and bottom rows denote respectively  $p=q=1$ ,  $p=q=2$  and  $p=q=3$ : (a.1–3)  $b=0$ , (b.1–3)  $b=1$ , (c.1–3)  $b=1.5$  and (d.1–3)  $b=4$

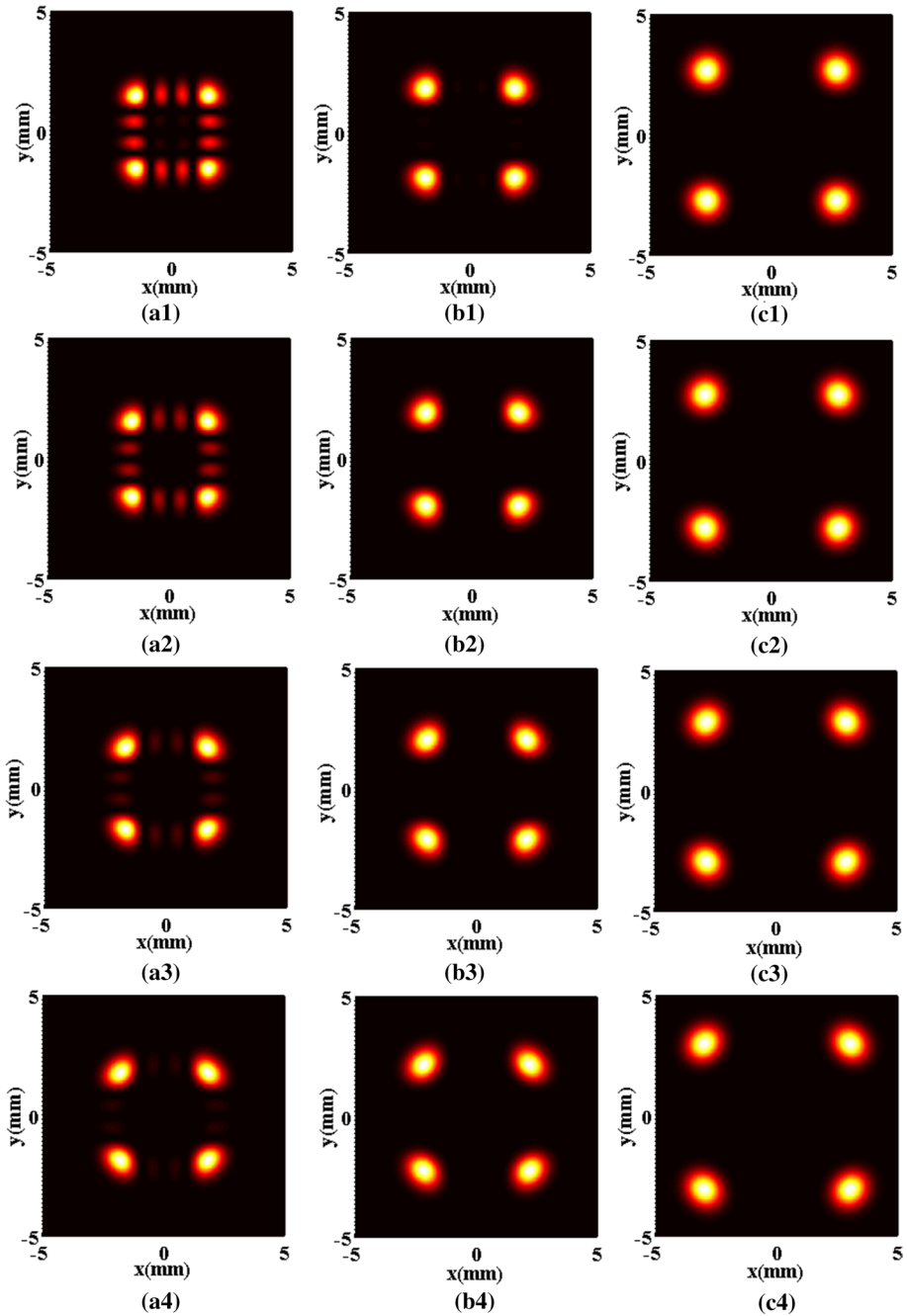
visible (see Fig. 1, columns (c–d)); the beam profile resembles closely to the four-petal beam (Duan and Lü 2006). One can also see a slight increasing of the inter-lobes space, and a narrowing of the lobes width when the beam orders  $(p, q)$  are increased (see the intensity distribution in the x-direction in the right side of Fig. 1).

Figure 2 illustrates the influence of the topological charge  $M$  on the vHChGB pattern. As can be seen, the main four petals slightly widen and elongate into an elliptical form under the effect of increasing the topological charge. In addition, one can note also an increasing of the inter-lobes space; this is clearly illustrated in Fig. 3 which presents the normalized intensity distribution in the x-direction.

### 3 Theoretical model

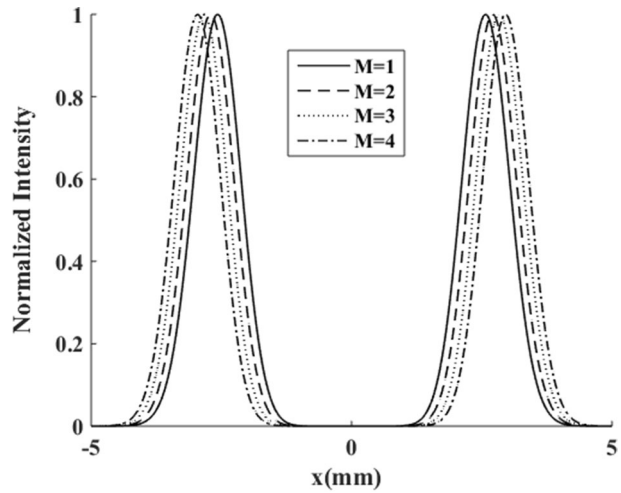
Within the framework of the paraxial approximation, the propagation of a laser beam through a paraxial ABCD optical system obeys the Collins formula (Collins 1970):

$$E(x, y, z) = \frac{ik}{2\pi B} e^{-ikz} \int_{-\infty}^{+\infty} \int_{-\infty}^{+\infty} E_0(x_0, y_0, 0) \exp \left\{ -\frac{ik}{2B} [A(x_0^2 + y_0^2) - 2(x_0 + yy_0) + D(x^2 + y^2)] \right\} dx_0 y_0, \quad (3)$$



**Fig. 2** The normalized intensity distribution of vHChG beam at the source plane with  $\omega_0 = 1$  mm and  $p=q=3$  for different  $b$ . The first, second, third and fourth rows denote respectively  $M=1$ ,  $M=2$ , 4 and  $M=6$ : (a.1–4)  $b=0$ , (b.1–4)  $b=1.5$  and (c.1–4)  $b=4$

**Fig. 3** The normalized intensity distribution of vHChG beam at the source plane with  $\omega_0=1$  mm,  $b=4$  and  $p=2$  for different topological charge values  $M$



where  $E_0(x_0, y_0, 0)$  and  $E(x, y, z)$  are the fields at the source ( $z=0$ ) and the receiver planes, respectively.  $z$  is the propagation distance,  $A, B,$  and  $D$  are the matrix elements of the optical system,  $k = \frac{2\pi}{\lambda}$  is the wave number and  $\lambda$  is the wavelength of radiation in vacuum.

Substituting from Eq. (1a) into Eq. (3), and recalling the binomial expansion (Gradshteyn and Ryzhik 1994)

$$(x_0 + iy_0)^M = \sum_{m=0}^M C_m^M x_0^m (iy_0)^{M-m} \tag{4a}$$

where

$$C_m^M = \frac{M!}{m!(M-m)!} \tag{4b}$$

we obtain

$$E(x, y, z) = \frac{ik}{2\pi B} e^{-ikz} e^{-\frac{iKD}{2B}(x^2+y^2)} \sum_{m=0}^M C_m^M (i)^{M-m} I_m(x) I_{M-m}(y), \tag{5a}$$

where

$$I_n(u) = \int_{-\infty}^{+\infty} u_0^n \cosh\left(b \frac{u_0}{\omega_0}\right) e^{-\alpha u_0^2 + \frac{ik}{B} u u_0} H_j\left(\frac{\sqrt{2}u_0}{\omega_0}\right) du_0 \tag{5b}$$

with  $u = x$  or  $y, r$  is an integer,  $j = p$  or  $q$  and  $\alpha$  is the auxiliary parameter defined as

$$\alpha = \frac{ikA}{2B} + \frac{1}{\omega_0^2}. \tag{5c}$$

Using the expansion form of the Hermite function  $H_j(\cdot)$  (Gradshteyn and Ryzhik 1994),

$$H_j(x) = \sum_{p=0}^{[j/2]} \frac{(-1)^p j!}{p!(j-2p)!} (2x)^{j-2p} \tag{6}$$

and recalling the following integral formula (Prudnikov et al. 1986; Belafhal et al. 2020)

$$\int_{-\infty}^{+\infty} x^n e^{-px^2+2qx} dx = e^{\frac{q^2}{p}} \sqrt{\frac{\pi}{p}} \left(\frac{1}{2i\sqrt{p}}\right)^n H_n\left(\frac{iq}{\sqrt{p}}\right) \tag{7}$$

then carrying on some tedious calculations, Eq. (5) turns out to be

$$E(x, y, z) = e^{-ikz} \frac{ik}{8\alpha B} \left(\frac{1}{2i\sqrt{\alpha}}\right)^M \left(\frac{\sqrt{2}}{i\omega_0\sqrt{\alpha}}\right)^{p+q} e^{\frac{b^2}{2\alpha\omega_0^2}} e^{-\left(\frac{ikD}{2B} + \frac{t^2}{4\alpha B^2}\right)(x^2+y^2)} \times \sum_{m=0}^M C_m^M(i)^{M-m} [f_{p,m}^+(x) + f_{p,m}^-(x)] [f_{q,M-m}^+(y) + f_{q,M-m}^-(y)], \tag{8}$$

where

$$f_{p,m}^\pm(x) = \sum_{s=0}^{\lfloor \frac{p}{2} \rfloor} \frac{p!}{s!(p-2s)!} \left(\frac{\alpha\omega_0^2}{2}\right)^s e^{\pm \frac{ikbx}{2\alpha B\omega_0}} H_{p+m-2s}\left(\frac{ik}{2B\sqrt{\alpha}}x \pm \frac{ib}{2\omega_0\sqrt{\alpha}}\right) \tag{9a}$$

and

$$f_{q,M-m}^\pm(y) = \sum_{h=0}^{\lfloor \frac{q}{2} \rfloor} \frac{q!}{h!(q-2h)!} \left(\frac{\alpha\omega_0^2}{2}\right)^h e^{\pm \frac{ikby}{2\alpha B\omega_0}} H_{q+M-m-2h}\left(\frac{ik}{2B\sqrt{\alpha}}y \pm \frac{ib}{2\omega_0\sqrt{\alpha}}\right) \tag{9b}$$

Equation (8) is the propagation formula of a vHChGB passing through a paraxial optical system.

This formula can be reduced in the following cases:

- (1) When  $b=0$ , Eq. (8) will give the diffracted vortex Hermite–Gaussian beam which can be expressed as

$$E(x, y, z) = \frac{ik}{2\alpha B} \left(\frac{1}{2i\sqrt{\alpha}}\right)^M \left(\frac{\sqrt{2}}{i\omega_0\sqrt{\alpha}}\right)^{p+q} e^{-ikz} e^{-\left(\frac{ikD}{2B} + \frac{t^2}{4\alpha B^2}\right)(x^2+y^2)} \sum_{m=0}^M C_m^M(i)^{M-m} f_{p,m}(x) f_{q,M-m}(y) \tag{10a}$$

where

$$f_{p,m}(u) = \sum_{s=0}^{\lfloor \frac{p}{2} \rfloor} \frac{p!}{s!(p-2s)!} \left(\frac{\alpha\omega_0^2}{2}\right)^s H_{p+m-2s}\left(\frac{ik}{2B\sqrt{\alpha}}u\right) \quad \text{with } u = x \text{ or } y \tag{10b}$$

Equation (10a) is consistent with the result of Ref. (Kotlyar et al. 2015).

**Fig. 4** Normalized intensity distribution of the vHChG beam with  $\omega_0=1$  mm,  $\lambda = 632.8$  nm and  $M=1$  for different propagation distance and different parameter values of  $b$ . the first three rows and the second ones denote respectively  $p=q=1$  and  $p=q=2$ . The first ( $z=0$ ), the second ( $z=z_R$ ) and the third row ( $z=15z_R$ ): (a.1–6)  $b=0$ , (b.1–6)  $b=0.1$ , (c.1–6)  $b=1.5$  and (d.1–6)  $b=4$

(2) In the case  $p = q = 0$ , Eq. (8) will give the propagation formula of the vChGB, which can be expressed as

$$E(x, y, z) = \frac{ik}{8\alpha B} \left( \frac{1}{2i\sqrt{\alpha}} \right)^M e^{-ikz} \sum_{m=0}^M C_m^M(i)^{M-m} e^{\frac{b^2}{2\alpha\omega_0^2}} e^{-\left(\frac{ikD}{2B} + \frac{k^2}{4\alpha B^2}\right)(x^2+y^2)} \times [f_m^+(x) + f_m^-(x)] [f_{M-m}^+(y) + f_{M-m}^-(y)] \tag{11a}$$

where

$$f_n^\pm(u) = e^{\pm \frac{ikbu}{2\alpha B\omega_0}} H_n \left( \frac{ik}{2B\sqrt{\alpha}} u \pm \frac{ib}{2\omega_0\sqrt{\alpha}} \right) \quad \text{with } u = x \text{ or } y \text{ and } n = m \text{ or } M - m \tag{11b}$$

The obtained equation is consistent with the result of Hricha et al. (2020).

Equation (10a) is consistent with the result of (Kotlyar et al. 2015).

(3) When  $p = q = b = 0$ , Eq. (8) will reduce to the hollow vortex Gaussian beam propagating through ABCD optical system (Zhou and Ru 2013), which can be written as

$$E(x, y, z) = \frac{ik}{2\alpha B} \left( \frac{1}{2i\sqrt{\alpha}} \right)^M e^{-ikz} e^{-\left(\frac{ikD}{2B} + \frac{k^2}{4\alpha B^2}\right)(x^2+y^2)} \sum_{m=0}^M C_m^M(i)^{M-m} \left[ H_m \left( \frac{ik}{2B\sqrt{\alpha}} x \right) H_{M-m} \left( \frac{ik}{2B\sqrt{\alpha}} y \right) \right]. \tag{12}$$

It is worth noting that the Eq. (12) is equivalent to Eq. (8) of Zhou et al. (2013) (if we take  $n=m/2$  in Zhou et al. (2013)) even if they are different in form.

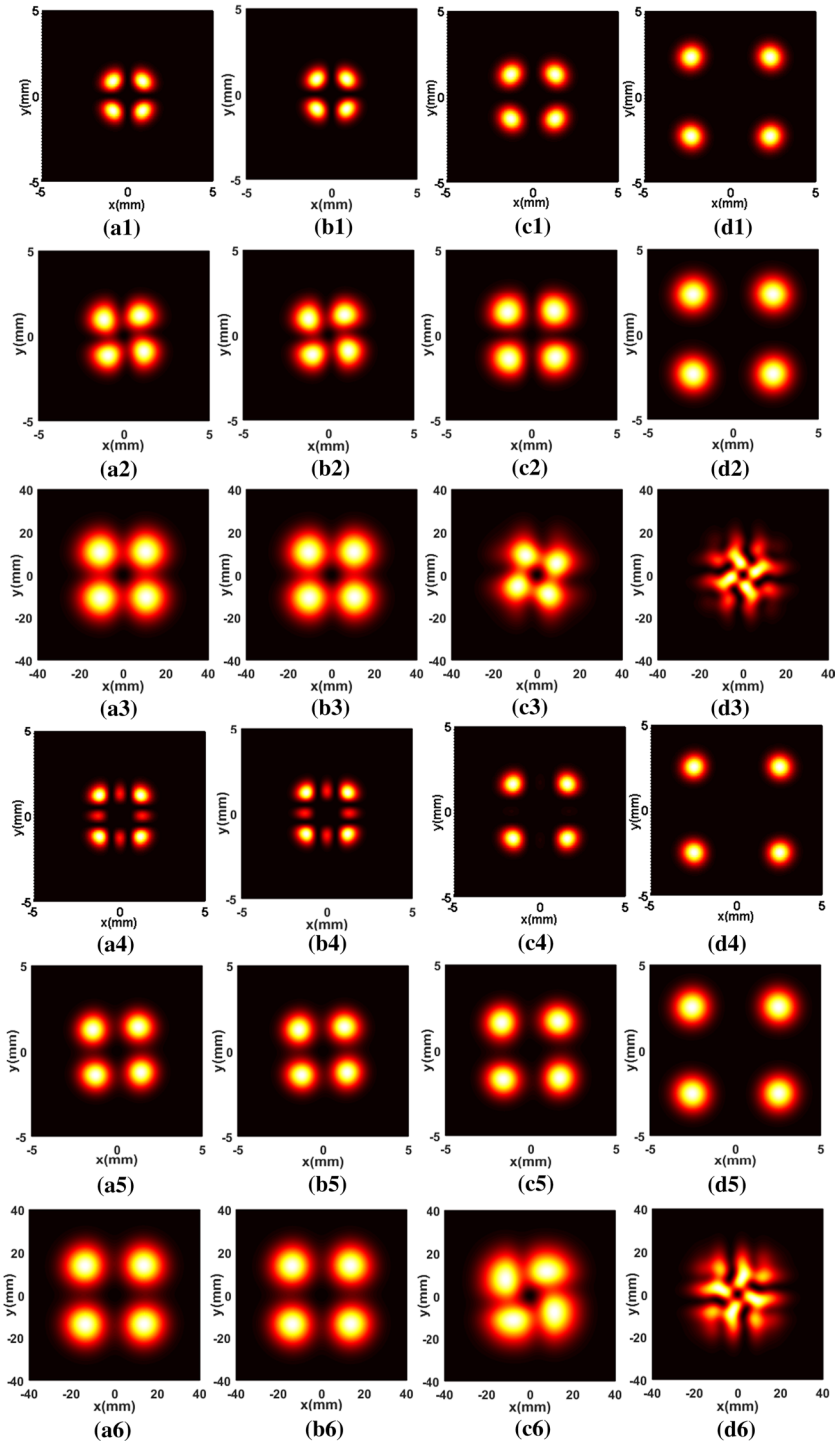
Equation (10a) is consistent with the result of Kotlyar et al. (2015).

### 4 Numerical results and discussions

Here, we investigate the evolution behavior of the vHChGB propagating in free space by calculating Eq. (8). The calculation parameters are taken as  $\lambda = 632.8$  nm,  $\omega_0 = 1$  mm and  $z_R = \frac{k\omega_0^2}{2}$  denotes the Gaussian Rayleigh length, which is used as the unit scale for the propagation distance. Figure (4) presents the typical intensity distributions of a vHChGB beam with  $M=1$  at the initial plane ( $z=0$ ), near field ( $z=z_R$ ) and far field ( $z=15z_R$ ), respectively, for different values of  $b$  and for  $p=q=1$  and  $p=q=2$ . From the plots of Fig. 4, it is shown that in near field, the main lobes widen gradually and the secondary lobes disappear completely (see plots (a.4)–(a.5); the field evolves into a four petal-like beam. In far-field, the size of the beam spot widens and the lobes bond. When  $b$  is large, the beam morphs into a “fan blades” structure whose pattern depends crucially on beam orders ( $p, q$ ) (see the plots (d.3)–(d.6)).

The effects of the beam orders ( $p, q$ ) and the topological charge  $M$  on the vHChG beam shape in far field are illustrated in Figs. (5) and (6). It is seen that for small  $b$ , the beam keeps the four-petal shape and the inter-lobes space increases with the increase of the beam orders ( $p, q$ ). Whereas for large  $b$  and with  $M=1$ , the four lobes overlap and morphs into fan blades-like





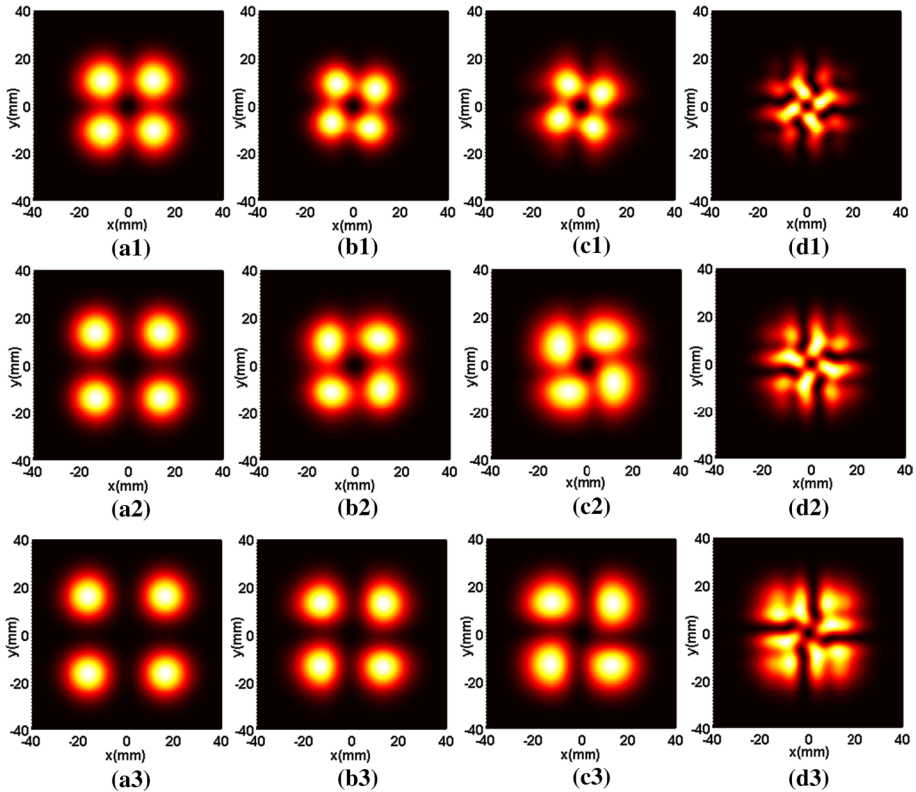


**Fig. 5** Normalized intensity distribution of the vHChG beam with  $\omega_0=1$  mm,  $\lambda = 632.8$  nm and  $M=1$  at  $z = 15z_R$  for different parameter values of  $b$ . The top, middle and bottom rows denote respectively  $p=q=1$ ,  $p=q=2$  and  $p=q=3$ : (a.1–3)  $b=0$ , (b.1–3)  $b=1$ , (c.1–3)  $b=1.5$  and (d.1–3)  $b=4$

pattern with a dark spot at the center for all the beam orders  $(p,q)$  (see Fig. 5(d.1–d.3)). For  $M=2$  and large values of  $b$  (see Fig. 6), the beam shape and the intensity at its center depend on the parity of  $p$  and  $q$ ; when  $(p,q)$  are odd the beam shape evolves into nine petals of mirror symmetry with a bright central core (see Fig. 6.(a4–c4)), whereas when  $(p,q)$  are even, the beam has four symmetrical wide spots with a dark central core (see Fig. 6.(b4–d4)).

Figure 7 illustrates the same characteristics as in Fig. 6 but with taking  $M=3$ . From the obtained plots, one can note the absence of the bright central core for all the orders presented; this is in accordance with the result obtained with  $M=1$  (see Fig. 5). This means that the parity of  $M$  is crucial for controlling the intensity at the beam’s center.

Figure 8 shows the effect of the topological charge  $M$  ( $M=5, 6$  and  $8$ ) on the beam shape in far field. One can clearly see that the main lobes elongate into elliptic form and separate with increasing the value of  $M$ . It follows from the above analysis that when the  $b$  parameter is large, the beam shape and the central area intensity of the diffracted vHChGB in far field depend significantly on the values and the parities of  $M, p$  and  $q$ .

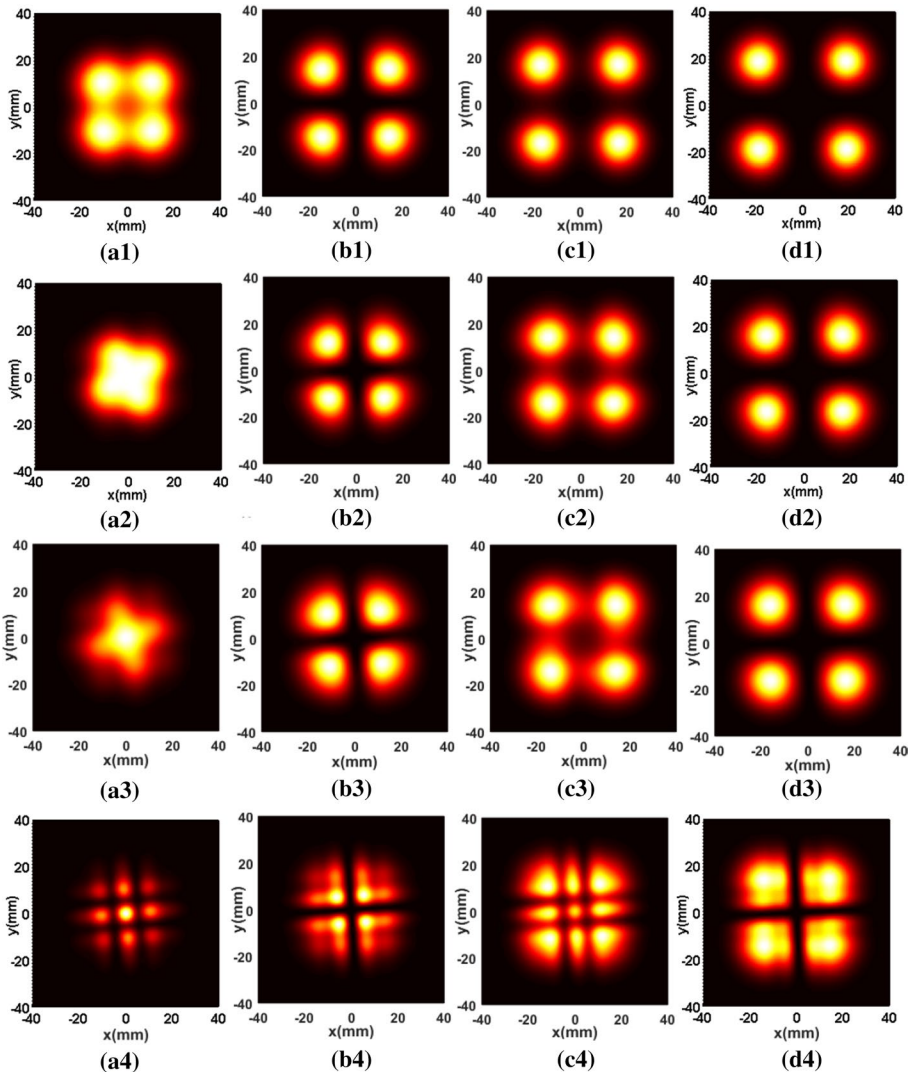


**Fig. 6** Normalized intensity distribution of the vHChG beam with  $\omega_0=1$  mm,  $\lambda = 632.8$  nm and  $M=2$  at  $z=15z_R$  for different values of  $p$  and  $q$ . The first, second, third and the fourth rows denote respectively  $b=0.1$ ,  $b=1$ ,  $1.5$  and  $b=4$ : (a.1–4)  $p=q=1$ , (b.1–4)  $p=q=2$ , (c.1–4)  $p=q=3$  and (d.1–4)  $p=q=4$

## 5 Conclusion

In summary, a vHChG beam is introduced. Based on the Collins diffraction integral, the propagation formula of the vHChGB through a paraxial ABCD optical system is derived. It emerges from illustrated examples that the beam parameters influence crucial the intensity pattern of the propagated vHChGB in free space. The shape of the vHChGB gradually

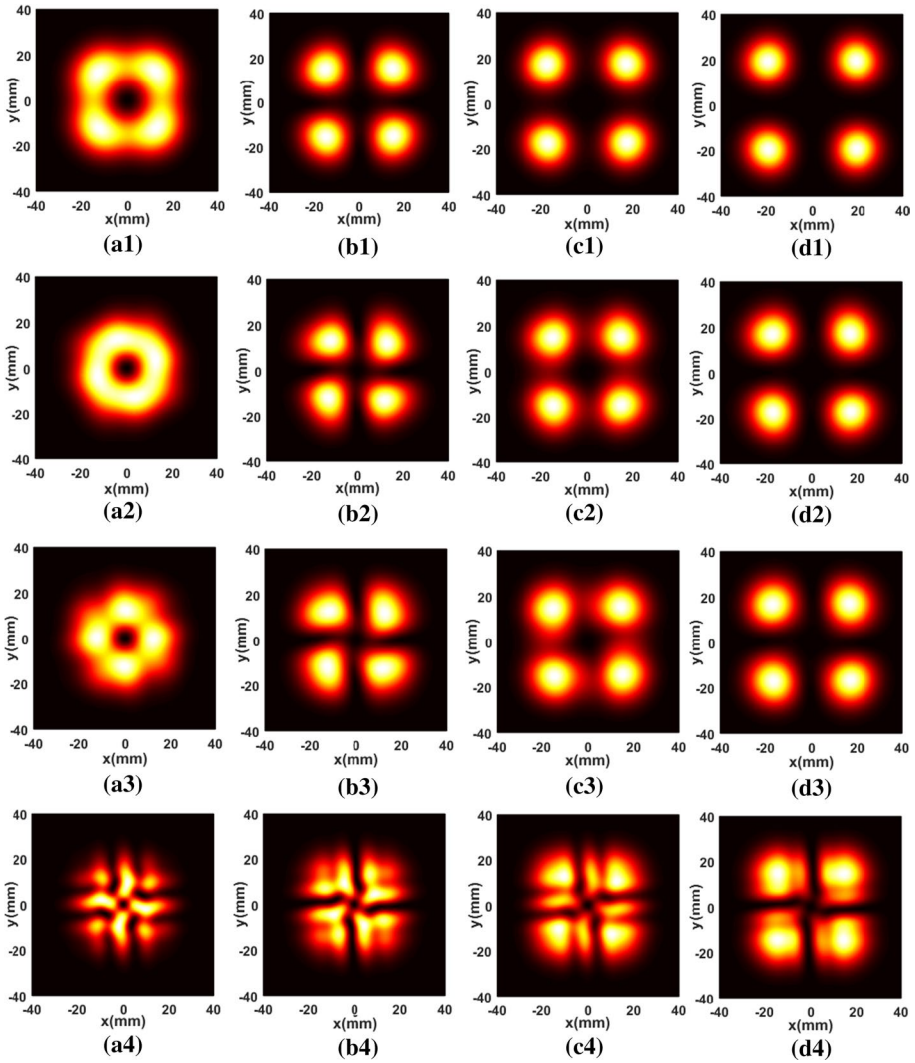
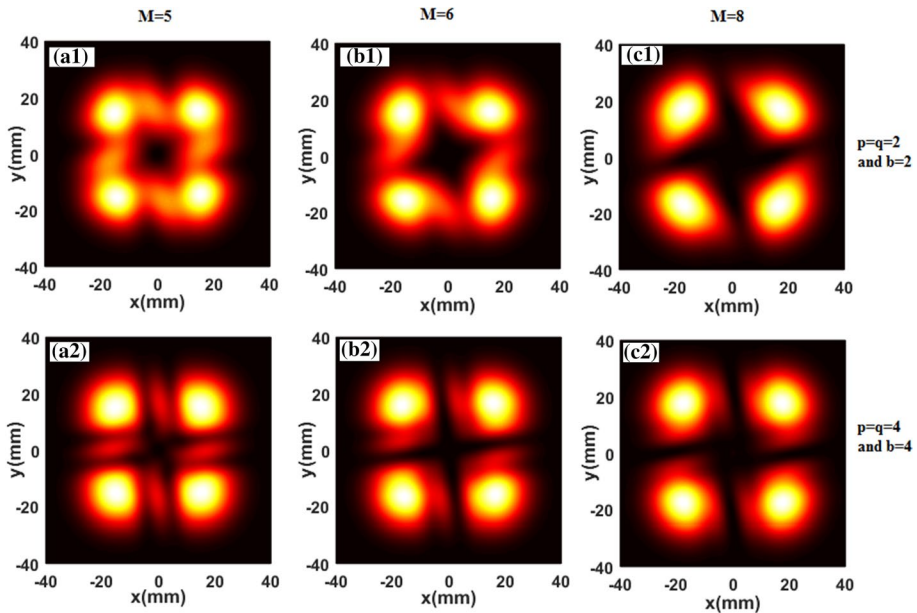


Fig. 7 The same as Fig. 6 except  $M=3$

changes upon propagating in near field, then morphs drastically in far-field. The size, the structure of the petals and the intensity of the central area of the beam can be controlled by adjusting the beam parameters. Our results may be useful in many applications where special intensity pattern of beam is privileged such as micro-optics, beam splitting techniques and optical communications.



**Fig. 8** Normalized intensity distribution of the vHChG beam with  $\omega_0 = 1$  mm and  $\lambda = 632.8$  nm at  $z = 15z_R$  for different values of  $M$ . The first and the second rows denote respectively  $b=2$  and  $p=q=2$ ,  $b=4$  and  $p=q=4$ . (a.1–2)  $M=5$ , (b.1–2)  $M=6$  and (c.1–2)  $M=8$

## References

- Allen, L., Beijersbergen, M.W., Spreeuw, R.J., Woerdman, J.P.: Orbital angular momentum of light and the transformation of Laguerre-Gaussian modes. *Phys. Rev. A*. **45**, 8185–8189 (1992)
- Arlt, J., Dholakia, K.: Generation of higher-order Bessel beams by use of an axicon. *Opt. Commun.* **177**, 297–301 (2000)
- Belafhal, A., Ibnchaikh, M.: Propagation properties of Hermite-cosh-Gaussian laser beams. *Opt. Commun.* **186**, 269–276 (2000)
- A. Belafhal, Z. Hricha, L. Dalil-Essakali, T. Usman, “A note on some integrals involving Hermite polynomials and their applications”. Accepted in advance mathematical models and applications (September 2020).
- Bishop, A.I., Nieminen, T.A., Heckenberg, N.R., Rubinsztein, H.: Optical microrhology using rotating laser-trapped particles. *Phys. Rev. Lett.* **92**, 198104 (2004)
- Cai, Y., Ge, D.: Propagation of various dark hollow beams through an aperture paraxial ABCD optical system. *Phys. Lett. A*. **357**, 72–80 (2006)
- Cai, Y., Lu, X., Lin, Q.: Hollow Gaussian beam and its propagation. *Opt. Lett.* **28**, 1084–1086 (2003)
- Casperson, L.W., Tovar, A.A.: Hermite-Sinusoidal-Gaussian beams in complex optical systems. *J. Opt. Am. A*. **15**, 954–961 (1998)
- Collins, S.A.: Lens-system diffraction integral written in terms of matrix optics. *J. Opt. Soc. Am.* **60**, 1168–1177 (1970)
- Dai, H.T., Liu, Y.J., Luo, D., Sun, X.W.: Propagation dynamics of an optical vortex imposed on an Airy beam. *Opt. Lett.* **35**, 4075–4077 (2010)
- Duan, K., Lü, B.: Four-petal Gaussian beams and their propagation. *Opt. Commun.* **261**, 327–331 (2006)
- Gradshteyn, I.S., Ryzhik, I.M.: Tables of integrals series and products, 5th edn. Academic Press, New York (1994)
- Guo, L., Tang, Z., Wan, W.: Propagation of four-petal Gaussian vortex beam through a paraxial ABCD optical system. *Optik* **125**, 5542–5545 (2014)

- Hricha, Z., Belafhal, A.: A comparative parametric characterization of elegant and standard Hermite-cosh-Gaussian beams. *Opt. Commun.* **253**, 231–241 (2005a)
- Hricha, Z., Belafhal, A.: Focusing properties and focal shift of hyperbolic-cosine-Gaussian beams. *Opt. Commun.* **253**, 242–249 (2005b)
- Hricha, Z., Yaalou, M., Belafhal, A.: Introduction of a new vortex cosine-hyperbolic-Gaussian beam and the study of its propagation properties in fractional fourier transform optical system. *Opt. Quant. Electron.* **52**, 296–302 (2020)
- Ibnchaikh, M., Dalil-Essakali, L., Hricha, Z., Belafhal, A.: Parametric characterization of truncated Hermite-cosh-Gaussian beams. *Opt. Commun.* **190**, 29–36 (2001)
- Ito, H., Nakata, T., Sakaki, K., Ohtsu, M., Lee, K.I., Jhe, W.: Laser spectroscopy of atoms guided by evanescent waves in micron-sized hollow optical fibers. *Phys. Rev. Lett.* **76**, 4500–4503 (1996)
- Karimi, E., Zito, G., Piccirillo, B., Marrucci, L., Santamato, E.: Hypergeometric Gaussian modes. *Opt. Lett.* **32**, 3052–3055 (2007)
- Kennedy, S.A., Szabo, M.J., Teslow, H., Porterfield, J.Z., Abraham, E.R.I.: Creation of Laguerre-Gaussian laser modes using diffractive optics. *Phys. Rev. A* **66**, 043801 (2002)
- Kotlyar, V.V., Almazov, A.A., Khonina, S.N., Soifer, V.A., Elfstrom, H., Turunen, J.: Generation of phase singularity through diffracting a plane or Gaussian beam by a spiral phase plate. *J. Opt. Soc. Am. A* **22**(5), 849–861 (2005)
- Kotlyar, V.V., Kovalev, A., Khonina, S.N., Skidanov, R.V., Soifer, V.A., Elfstrom, H., Tossavainen, N., Turunen, J.: Diffraction of conic and Gaussian by spiral phase plate. *Appl. Opt.* **45**, 2656–2665 (2006)
- Kotlyar, V.V., Skidanov, R.V., Khonina, S.N., Soifer, V.A.: Hypergeometric modes. *Opt. Lett.* **32**(7), 742–744 (2007)
- Kotlyar, V.V., Kovalev, A.A., Porfirev, A.P.: Vortex Hermite-Gaussian laser beams. *Opt. Lett.* **40**(5), 701–704 (2015)
- Kuga, T., Torii, Y., Shiokawa, N., Hirano, T., Shimizu, Y., Sasada, H.: Novel optical trap of atoms with a doughnut beam. *Phys. Rev. Lett.* **78**, 4713–4716 (1997)
- Liu, H., Lü, Y., Xia, J., Pu, X., Zhang, L.: Flat-topped vortex hollow beam and its propagation properties. *J. Opt.* **17**(7), 075606–075608 (2015)
- McGloin, D., Dholakia, K.: Bessel beams: diffraction in new light. *Contemp. Phys.* **46**, 15–28 (2005)
- Monin, E.O., Ustinov, A.V.: The transformation of Hermite-Gauss beams with embedded optical vortex by lens system. *J. Phys. Conf. Ser.* **1038**(1), 012039–012045 (2018)
- Oemrawsingh, S.S.R., van Houwelingen, J.A.W., Eliel, E.R., Woerdman, J.P., Versteegen, E.J.K., Kloosterboer, J.G., Hooft, G.W.: Production and characterization of spiral phase plates for optical wavelengths. *Appl. Opt.* **43**(3), 688–694 (2004)
- Paterson, L., MacDonald, M.P., Arlt, J., Sibbett, W., Bryant, P.E., Dholakia, K.: Controlled rotation of optically trapped microscopic particles. *Science* **292**(5518), 912–914 (2001)
- A.P. Prudnikov, Y.A. Brychkov, O.I. Marichev, 1986 URSS Academy of sciences, “Integrals and series”. Overseas Publishers Association.
- Rubinsztein-Dunlop, H., et al.: Roadmap on structured light. *J. Opt.* **19**(1), 013001 (2017)
- Siviloglou, G.A., Christodoulides, D.N.: Accelerating finite Airy beams. *Opt. Lett.* **32**, 979–981 (2007)
- Siviloglou, G.A., Broky, J., Dogariu, A., Christodoulides, D.N.: Observation of accelerating Airy beams. *Phys. Rev. Lett.* **99**, 213901–213904 (2007)
- Skidanov, R.V., Khonina, S.N., Morosov, A.A.: Optical rotation of microparticles in hypergeometric laser beams with a diffractive optical element with multilevel microrelief. *J. Opt. Techn.* **80**, 585–589 (2013)
- Torok, P., Munro, P.R.T.: The use of Gauss-Laguerre vector beams in STED microscopy. *Opt. Exp.* **12**(15), 3605–3617 (2004)
- Tovar, A.A., Casperson, L.W.: Production and propagation of Hermite-sinusoidal-Gaussian laser beams. *J. Opt. Am. A* **15**, 2425–2432 (1998)
- Vaity, P., Rusch, L.: Perfect vortex beam: fourier transform of Bessel beam. *Opt. Lett.* **40**(4), 742–744 (2015)
- Vallone, G.: On the properties of circular beams: normalization, Laguerre-Gauss expansion, and free-space divergence. *Opt. Lett.* **40**(8), 1717–1720 (2015)
- Wang, J., Yang, J.Y., Willner, A.E.: Terabit free-space data transmission employing orbital angular momentum multiplexing. *Nat. Phot.* **6**(7), 488–412 (2012)
- Wang, Y.B., Yang, Z.J., Pang, Z.G., Li, X.L., Zhang, S.M.: Shape-variable four-petal Gaussian breathers in strongly nonlocal nonlinear media. *Res. Phys.* **15**, 1023583–1023588 (2019)
- Zhou, G.: Propagation of a Lorentz-Gauss beam through a misaligned optical beam. *Opt. comm.* **283**(7), 1236–1243 (2010)
- Zhou, G., Ru, G.: Propagation of Lorentz-Gauss vortex beam in a turbulent atmosphere. *Prog. In Electromag. Res.* **143**, 143–163 (2013)

Zhou, G., Cai, Y., Dai, C.: Hollow vortex Gaussian beams. *Sci. Chin.* **56**(5), 896–903 (2013)

Zhou, Y., Zhou, G., Chen, R.P.: Propagation of hollow vortex Gaussian beam in SNNM. *Laser Phys.* **28**(10), 105003–105008 (2018)

**Publisher's Note** Springer Nature remains neutral with regard to jurisdictional claims in published maps and institutional affiliations.